Journal of Photochemistry and Photobiology 9 (2022) 100098

Contents lists available at ScienceDirect

Journal of Photochemistry and Photobiology

journal homepage: www.sciencedirect.com/journal/journal-of-photochemistry-and-photobiology

Ir(III)-Naphthoquinone complex as a platform for photocatalytic activity

Walter D. Guerra [a,*], Hannah J. Sayre [b], Hunter H. Ripberger [b], Emmanuel Odella [a], Gregory D. Scholes [b], Thomas A. Moore [a], Robert R. Knowles [b,**], Ana L. Moore [a,*]

[a] School of Molecular Sciences, Arizona State University, Tempe, AZ 85287, USA
[b] Department of Chemistry, Princeton University, Princeton, New Jersey 08544, USA

ARTICLE INFO

Keywords:
Artificial photosynthesis
heteroleptic Ir(III) complexes
photocatalyst
quinones
electron transfer (ET)

ABSTRACT

Inspired by the primary events that take place in Photosystem II (PSII), we designed and synthesized a heteroleptic Ir(III) complex featuring an attached naphthoquinone (NQ) as an electron transfer (ET) auxiliary reminiscent of the plastoquinone electron acceptor in PSII. In this design, NQ is covalently attached to the 2,2′-bipyridyl (bpy) ligand of $[Ir(dF(CF_3)ppy)_2(bpy)][PF_6]$, ($dF(CF_3)ppy$ = 2-(2,4-difluorophenyl)-5-(trifluoromethyl) pyridine). Following excitation of the photocatalyst ($[Ir(dF(CF_3)ppy)_2(bpy\text{-}NQ)][PF_6]$), reduced NQ ($NQ^{\bullet -}$) was observed in transient absorption spectroscopy. This novel catalyst has potential applications in oxidative and reductive photocatalytic processes.

1. Introduction

Electron transfer (ET) reactions are ubiquitous processes in nature and technology. The importance and intricacy of ET reactions in nature have inspired their investigation in simplified model systems [1,2]. Such model systems continue to be important in the development of artificial photosynthetic systems containing electron donor-acceptor moieties as well as light-harvesting antennas and photoprotective features to explore in detail the combination of factors that nature uses to harvest and store solar energy. In this context, one of the widely explored approaches is the use of covalently linked chromophore-electron donor--acceptor systems [1–8]. Also, a large variety of chromophore-electron acceptor complexes based on transition-metal and non-innocent quinone-related ligands have been reported. *O*-quinones and their reduced forms can chelate metals through the adjacent oxygen atoms behaving as bidentate catechol ligands. Such systems are the focus of research due to their interesting redox, photophysical, and photochemical properties [9–26].

Another method of mimicking nature's elementary ET processes is by coordinating a quinone to an (NˆN) bidentate ligand (*e.g.* bipyridine, bpy) in a metal complex. A series of ruthenium(II) polypyridyl complexes having a covalently attached benzoquinone (BQ) [27], anthraquinone (AQ) [28–32], or a fused quinone-type system[33,34] have been prepared and characterized. In these dyads, the photoinduced ET mechanism was investigated and initial assessment of driving-force, solvent polarity, and influence of hydrogen bonding on the overall photoinduced ET process was evaluated [27–34].

Heteroleptic $[Ir(C\hat{}N)_2(N\hat{}N)]^+$ complexes, where CˆN is a cyclometalating 2-phenylpyridyl (ppy) ligand and NˆN is a 1,2-diimine ancillary ligand (*e.g.* bpy), are well-known constructs (example in Chart 1, compound **1**) due to their modular synthesis, enhanced photostability, and long-lived triplet excited states [35–38]. The cyclometallated ligands generate a large ligand-field splitting, resulting in significant variability in the emission of reported Ir(III) complexes [39]. Moreover, the photophysical properties of the heteroleptic iridium complexes can be synthetically engineered. Tuning the HOMO and LUMO energies and consequently modifying the gap between them is possible through incorporation of substitutions on the cyclometalating and/or ancillary ligands [38,40,41].

Additionally, a triad comprised of a triarylamine electron donor, Ir (III) photosensitizer and AQ electron acceptor has been studied [31,42]. A charge-separated state with a lifetime in the microsecond regime was observed [31]. Excited state lifetimes of Ru(II)-AQ dyads, as measured by time-resolved luminescence experiments, were in the same range [30].

In this report, we describe the design, synthesis, electrochemical, and preliminary photophysical observations of a novel heteroleptic Ir(III) complex having a naphthoquinone (NQ) covalently attached to the ancillary bpy ligand. This dyad, $[Ir(dF(CF_3)ppy)_2(bpy\text{-}NQ)][PF_6]$ (**2**) is shown in Chart 1, together with a reference Ir(III) complex lacking the

* Corresponding author at: School of Molecular Sciences, Arizona State University, Tempe, Arizona 85287, USA.
** Corresponding author at: Department of Chemistry, Princeton University, Princeton, New Jersey 08544, USA.
E-mail addresses: wguerra1@asu.edu (W.D. Guerra), rknowles@princeton.edu (R.R. Knowles), amoore@asu.edu (A.L. Moore).

https://doi.org/10.1016/j.jpap.2021.100098

Available online 21 December 2021

NQ moiety, [Ir(dF(CF$_3$)ppy)$_2$(bpy)][PF$_6$] (**1**). Reports regarding polypyridyl iridium photocatalysts having attached quinone moieties are limited with little electrochemical and photophysical characterization [43]. Upon excitation of the Ir(III) complex **2** ET generates a long-lived state with the negative charge on the NQ moiety ($NQ^{\bullet-}$). Preliminary results of time resolved emission and absorption spectroscopies indicate that this long-lived state is probably formed in a bimolecular process. This photocatalyst would feature the reducing and oxidizing centers on different catalytic molecules and could be further developed for use in photocatalytic redox processes.

2. Results and discussion

2.1. Synthesis of complex 2

The synthesis of dyad **2** is shown in Scheme 1, divided into the construction of the substituted bpy ligand (Scheme 1-A), followed by complexation with the iridium precursor and final oxidation to obtain **2** (Scheme 1-B). Starting with methyl 5,8-dimethoxy-2-naphthoate (**A**) under basic conditions, the corresponding methyl ester hydrolysis was achieved. Naphthoic acid **B** was isolated in excellent yield (90%). Employing a direct amidation reaction (EDCI and DMAP in CH_2Cl_2) [44], bipyridine amide **D** was obtained in good yield (76%) by the reaction of acid **B** and commercially available bipyridine amine **C** (Scheme 1-A).

Amide **D** was used as a ligand in the complexation with Ir(III) precursor **E** under previously reported conditions[45,46] to obtain compound **F**, still with the protected naphthoquinone as a dimethoxynaphthalene. Final oxidation of **F** yields the desired target molecule **2** employing CAN (ceric ammonium nitrate) [47]. Ir(III) photocatalyst **2** was isolated with 58% yield for the final two steps (complexation and oxidation, Scheme 1-B). Other synthetic alternatives were explored with the prior oxidation of bipyridine derivative **D** followed by a complexation process, but poor yields and purification issues were observed. The complete synthetic procedure and NMR characterization of all intermediates (**B, D**, and **F**) and final complex **2** are provided in the Supporting Information (SI), Sections 1-2.

2.2. Electrochemical characterization

To evaluate the feasibility of the photoinduced ET processes, an accurate assignment of the electrochemical behavior of photocatalyst **2** is needed. Cyclic voltammetry (CV) is a useful technique to measure the redox potentials of different redox-active moieties within the photocatalyst. The CV of **2** has been performed in degassed acetonitrile (CH_3CN) solution using tetrabutylammonium hexafluorophosphate ($TBAPF_6$, 0.1 M) as supporting electrolyte. Midpoint potentials ($E_{1/2}$) for all the compounds studied were determined as the average of anodic and cathodic peak potentials ($E_{1/2} = (Ep_a + Ep_c)$ / 2) and are summarized in Table 1. The corresponding assignments are based on comparison with data obtained for reference compounds **1**[48] (the photocatalyst without the appended NQ) and NQ under the same conditions.

The electrochemical study of **2** is shown in Fig. 1, highlighting the window between −1.5 V to +2.0 V *vs* $Fc^{+/0}$ in panel A and the larger reduction window ($E > -2.3$ V *vs* $Fc^{+/0}$) in panel B. Additionally, the complete CV is shown in Fig. S11 combined with the CV of model NQ. The CV of **2** (Fig. 1-A, Table 1), shows the one-electron oxidation of the metal center (Ir^{IV}/Ir^{III} redox couple) at 1.34 V *vs* $Fc^{+/0}$ ($\Delta E_p = 90$ mV). In the case of the photocatalyst reference **1**, lacking the NQ moiety, this oxidation is observed at 1.35 V *vs* $Fc^{+/0}$ ($\Delta E_p = 80$ mV, Fig. S11) [41]. These results suggest that modification of the bpy ligand with the attached NQ does not affect the Ir^{IV}/Ir^{III} redox couple.

In contrast to the anodic region, the cathodic portion of the CV is more complex because several reductions occur (Fig. 1-B). The intricacy of the reduction behavior results from the multiple reduction processes involving the NQ, the bpy, and the ppy. Many examples of ruthenium

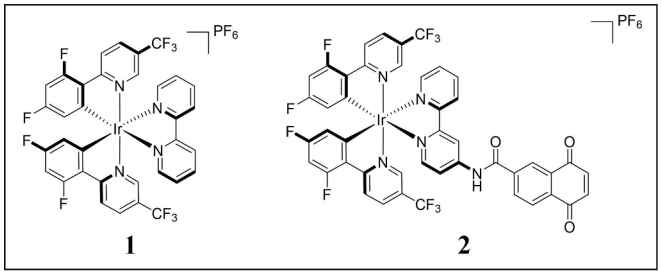

Chart 1. Molecular structures of [Ir(dF(CF$_3$)ppy)$_2$(bpy)][PF$_6$] (**1**, reference compound) and [Ir(dF(CF$_3$)ppy)$_2$(bpy-NQ)][PF$_6$] (**2**, target molecule).

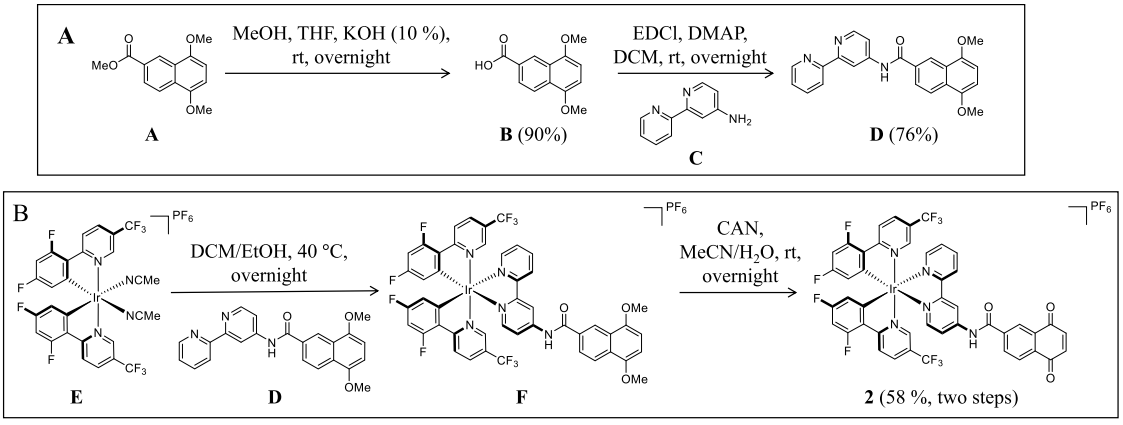

Scheme 1. General synthetic scheme for preparation of [Ir(dF(CF$_3$)ppy)$_2$(bpy-NQ)][PF$_6$] (**2**). A) Synthesis of bpy ligand **D**. B) Complexation and oxidation to achieve compound **2**.

Table 1
Electrochemical data for complex **2** and model compounds (**1** and NQ).

Compounds	$E_{1/2}$[a]/V (ΔE_p[b]/mV) $Ir^{III/IV}$	$NQ/NQ^{\bullet-}$	$NQ^{\bullet-}/NQ^{2-}$	$bpy^{0/-}$	$dF(CF_3)ppy^{-/2-}$
Complex **2**	1.34 (90)	−1.07 (70)	−1.71 (100)	~ −1.59[d]	−1.93 (70)
Complex **1**[c]	1.35 (80)			−1.64 (60)	−2.04[d]
NQ		−1.07 (70)	−1.71 (100)		

[a] Half-waves potential in degassed CH_3CN, 0.1 M $TBAPF_6$ *vs* Fc^+/Fc.
[b] ΔE_p measured at $\nu = 100$ mV s^{-1}.
[c] Data extracted from Ref [48].
[d] Irreversible cathodic peak.

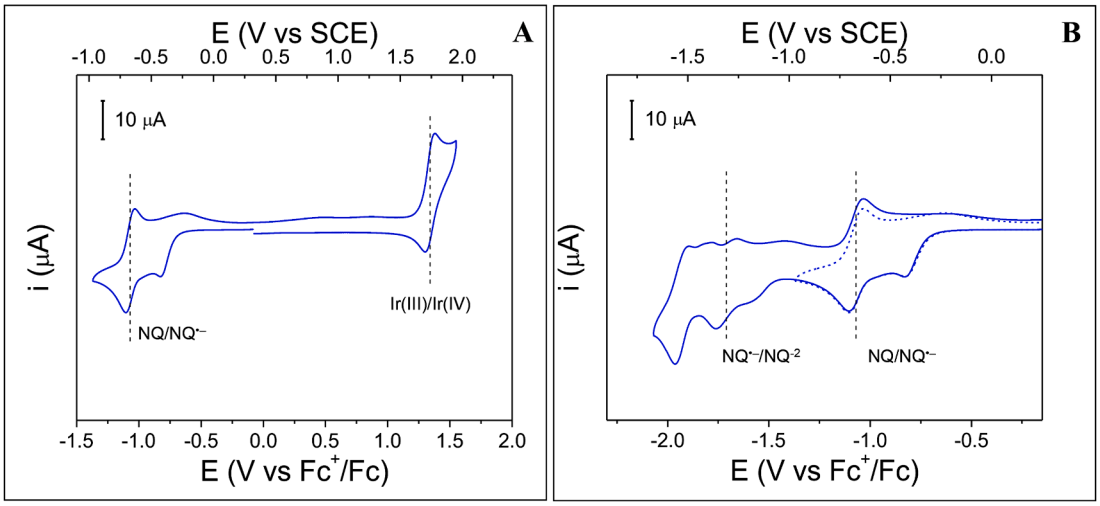

Fig. 1. A) Cyclic voltammogram of **2** recorded at potentials greater than the switching potential −1.37 V *vs* $Fc^{+/0}$. B) Cyclic voltammogram of **2** in the cathodic region recorded at potentials greater than the switching potential −1.37 V *vs* $Fc^{+/0}$ (dashed blue line) and greater than −2.07 V *vs* $Fc^{+/0}$ (solid blue line). Experimental conditions: 1 mM of the photocatalyst **2**, 0.1 M $TBAPF_6$ supporting electrolyte in degassed CH_3CN. WE: glassy carbon. Pseudo RE: Ag wire (ferrocene as internal reference). CE: Pt wire. Scan rate, 100 mV s^{-1}.

complexes bearing AQ moieties show similar complexity in their reduction profiles [28,30]. However, it is possible to assign the redox wave occurring at −1.07 V *vs* $Fc^{+/0}$ ($\Delta E_p = 70$ mV) in **2** to the $NQ/NQ^{\bullet-}$ redox couple (Fig 1. and Table 1). Additionally, more negative processes could be tentatively assigned to the reduction of the bpy ligand ($bpy^{0/-}$, cathodic peak at ~ −1.59 V *vs* $Fc^{+/0}$), the second reduction process of the NQ ($NQ^{\bullet-}/NQ^{2-}$, redox wave at −1.71 V *vs* $Fc^{+/0}$ ($\Delta E_p = 100$ mV)) and the ppy moiety ($dF(CF_3)ppy^{-/2-}$, reduction wave at −1.93 V *vs* $Fc^{+/0}$ ($\Delta E_p = 70$ mV), Fig. S11). This proposed assignment is based on both models, compound **1** and NQ (Table 1), and on previously reported data [48–50].

2.3. Steady state absorption and emission

Steady state absorption and emission data for both photocatalysts **1** and **2** are shown in Fig. 2 and summarized in Table 2. Both complexes demonstrate similar steady-state absorption and emission features except for notable emission quenching in **2**. Photocatalysts **1** and **2** demonstrate π→π* transitions in the UV, with maxima at 265 and 275 nm, respectively. Both photocatalysts have lowest energy transitions centered around 400 nm assigned to an Ir(d)→ppy(π*) metal-to-ligand charge transfer ($^1MLCT_{ppy}$) transition that is sometimes called a ligand centered (LC) ppy π→π* transition because there is significant molecular orbital mixing between the metal and ppy ligand in the HOMO [35]. Rapid intersystem crossing produces the corresponding triplet ($^3MLCT_{ppy}$) excited state.

Depending on ligand environment, similar heteroleptic Ir(III) complexes emit either from the $^3MLCT_{ppy}$ state or undergo a ppy(π*)→bpy(π*) ligand-to-ligand charge transfer (LLCT) to generate an emissive $^3MLCT_{bpy}$ state [41]. Photocatalyst **1** emits from the $^3MLCT_{ppy}$ state [48]. Emission quantum yields of photocatalysts **1** and **2** upon $\lambda^{irr} = 400$ nm in CH_3CN were determined relative to $Ir(ppy)_3$ ($\Phi = 0.97$ in MeTHF) [48]. The similarity in emission spectra between **1** and **2** suggests both photocatalysts emit from the same $^3MLCT_{ppy}$ state. The decrease in the emission quantum yield from $\Phi = 0.87$ for **1** to $\Phi = 0.20$ for **2** indicates significant quenching by the bpy ligand bearing the quinone substituent,

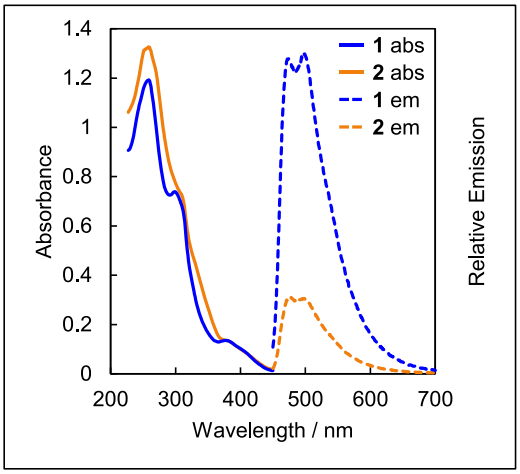

Fig. 2. Electronic absorption (abs) and emission (em) of complexes **1** and **2** in CH_3CN, $\lambda^{irr} = 400$ nm.

Table 2
Summary of emission properties of **1** and **2** in CH_3CN upon $\lambda^{irr} = 400$ nm.

Complex	λ_{em} / nm	Φ
1	480, 505	0.87
2	480, 505	0.20

indicating an additional relaxation pathway from the $^3MLCT_{ppy}$ excited state is available for **2**. As discussed below, the additional pathway is assigned to ppy(π*)→bpy(π*) LLCT followed by complex, and at this preliminary stage unassigned to electron transfer processes, to form a long lived $NQ^{\bullet-}$. The formation of a long lived species from a biomolecular process implies there must be the concomitant formation of a complex with Ir(IV). Unfortunately, this species is not detected because there is no definitive spectroscopic signature in the transient absorption spectrum for the conversion of Ir(III) to Ir(IV).

2.4. Density functional theory calculations

The electronic structure of photocatalyst **2** was investigated with qualitative density functional theory (DFT) calculations using the Gaussian 16 software package [48]. Calculations were performed using the wB97XD functional with a 6–311G+(d,p)/LanL2DZ (Ir) split basis set in a polarizable continuum solvent model (PCM, CH_3CN). Functionals containing dispersion and long-range corrections, like wB97XD, are better suited to handle the modeling of charge-transfer processes[51, 52] and the chosen basis sets have been employed in computational studies of other iridium complexes [41,48].

In line with other heteroleptic $[Ir(C^N)_2(N^N)]^+$ complexes, these calculations showed the HOMO predominantly composed of the Ir(III) d orbitals and π orbitals on the cyclometalated ligand (Fig. S12). In contrast, the LUMO is calculated to be largely π* orbitals on the appended quinone moiety (Fig. S13). The position of the LUMO is consistent with the quinone being easier to reduce than the bipyridine (see Electrochemical Characterization, Section 2.2). Charge separation in the triplet excited state of the complex would produce an intramolecular ^3CSS with an oxidized metal center and reduced quinone. The generated spin density plot of the optimized geometry of the triplet state of **2** illustrates this charge separation, with spin density localized on both the Ir center and cyclometalated ligand, as well as on the quinone (Fig. S14).

2.5. Visible transient absorption measurements

In preliminary experiments, the photophysics of photocatalyst **2** were explored with visible transient absorption spectroscopy. All transient absorption experiments were performed in deoxygenated ~0.2 mM solution in CH_3CN with excitation centered at $\lambda^{irr} = 400$ nm.

Excitation of **2** produces an excited state species with absorption at 485 nm similar to the excited state absorption reported for **1** [53]. After ~1 microsecond the excited state absorption spectrum is clearly discernable from spectra at earlier times (Fig. S15) and persists essentially unchanged, except for a decay in intensity, for hundreds of microseconds (Fig. 3-A). This long-lived feature strongly resembles the spectroelectrochemical reduction of the NQ ligand (Fig. 3-B). In contrast, the longest-lived transient species in **1** is the $^3MLCT_{ppy}$ state with a lifetime of 2.8 μs [48,53,54].

Due to its exceptionally long lifetime, unprecedented for an intramolecular charge-separated state [2,55], the spectrum observed at long times is tentatively assigned to a bimolecular charge-separated species arising from electron transfer from the $^3MLCT_{bpy}$ state or from the intramolecular charge separated state (Ir(IV)bpy$NQ^{\bullet-}$) to a neighboring ground state molecule of **2** in a diffusion-control process. The bimolecular process involved in the decay requires the resulting ions bearing the Ir(IV) metal and $NQ^{\bullet-}$ moiety diffuse through solution before charge recombination, extending the time for the $NQ^{\bullet-}$ species to hundreds of microseconds. Additional transient absorption experiments including solvent, concentration- and laser-power dependence studies are needed to further characterize charge separation and recombination [56,57].

3. Conclusions

A bioinspired, heteroleptic Ir(III) complex with an attached NQ has been synthesized, electrochemically characterized and the formation of a long-lived charge separated species observed. The synthesis of $[Ir(dF(CF_3)ppy)_2(bpy\text{-}NQ)][PF_6]$ (**2**) involves the construction of the substituted bpy with the protected NQ, followed by complexation and oxidation to achieve the target complex in good overall yield. Electrochemical characterization of **2** showed that the covalently attached NQ does not affect the Ir^{IV}/Ir^{III} redox couple, and the complex reduction profile can be understood based on the redox properties of known model compounds.

The emission quantum yield of **2** is quenched compared to the reference complex without the attached NQ. Transient absorption

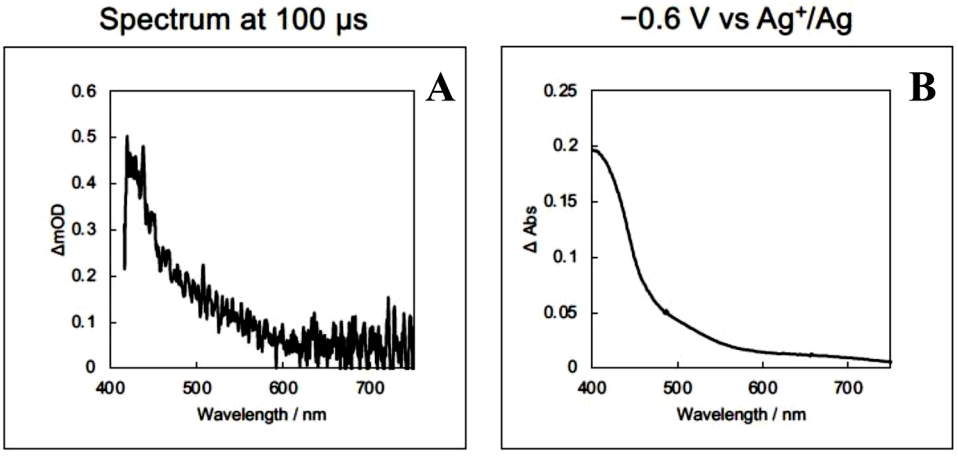

Fig. 3. (A) Transient absorption spectra of **2** in CH_3CN upon $\lambda^{irr} = 400$ nm. Spectrum at 100 microseconds from 2D graph (Fig. S15). (B) Visible spectroelectrochemistry spectrum of **2** in 0.1 M $TBAPF_6$ /CH_3CN upon −0.6 V *vs* Ag^+/Ag (~1 V *vs* Fc^+/Fc) applied potential.

measurements indicate that excitation of **2** results in the formation of a charge-separated state where the negative charge is localized on an NQ moiety. The long-lived, charge-separated state is most likely produced bimolecularly, involving an initially formed intramolecular $^{3}MLCT_{bpy}$ state or from the intramolecular chargeseparated state (Ir(IV)bpyNQ$^{\bullet-}$) and a ground state complex. The possibility that those states are involved in a bimolecular process at the low concentrations of the catalyst on the microsecond time scale is a good predictor for the involvement of catalyst **2** in initiating redox processes, which require a collision complex formed by a "photo activated" catalyst molecule and a substrate molecule at much higher concentration. Synthetically useful photocatalytic reactions such as olefin hydroamination [58], alkene carboamination [59], ketyl-olefin cyclization [60], among others [61]. can be imagined. Furthermore, **2** opens the door to the synthesis of substituted quinones having hydrogen-bonded proton donors, a feature that would promote proton-coupled electron transfer (PCET) processes. In a recent study, such a strategy has proven effective in improving the quantum yield of a photoreductive process [48].

4. Author information

Corresponding Authors: Walter D. Guerra: School of Molecular Sciences, Arizona State University, Tempe, Arizona 85287, United States; ORCID: 0000-0003-0712-2740. Email: wguerra1@asu.edu.**Ana L. Moore**: School of Molecular Sciences, Arizona State University, Tempe, Arizona 85287, United States; ORCID: 0000-0002-6653-9506; Email: amoore@asu.edu. **Robert R. Knowles**: Department of Chemistry, Princeton University, Princeton, New Jersey 08544, United States; ORCID: 0000-0003-1044-4900; Email: rknowles@princeton.edu. **Authors:** Hannah J. Sayre: Department of Chemistry, Princeton University, Princeton, New Jersey 08544, United States; ORCID: 0000-0002-3214-4899. Current address: Department of Chemistry and Chemical Biology, Northeastern University, Boston, Massachusetts 02115. Hunter H. Ripberger: Department of Chemistry, Princeton University, Princeton, New Jersey 08544, United States; ORCID: 0000-0002-3146-9579. Emmanuel Odella: School of Molecular Sciences, Arizona State University, Tempe, Arizona 85287, United States; ORCID: 0000-0002-7021-400X.Gregory D. Scholes: Department of Chemistry, Princeton University, Princeton, New Jersey 08544, United States; ORCID: 0000-0003-3336-7960.Thomas A. Moore: School of Molecular Sciences, Arizona State University, Tempe, Arizona 85287, United States; ORCID: 0000-0002-1577-7117.

5 Declaration of Competing Interest

The authors declare that they have no known competing financial interests or personal relationships that could have appeared to influence the work reported in this paper.

6 Acknowledgments

The authors wish to thank Joseph S. Beckwith for discussion of excited state dynamics. This work was supported as part of BioLEC (Bioinspired Light-Escalated Chemistry) an Energy Frontier Research Center funded by the U.S. Department of Energy, Office of Science, Basic energy Sciences under Award #DE-SC0019370.

7 Supplementary materials

Supplementary material associated with this article can be found, in the online version, at doi:10.1016/j.jpap.2021.100098. Supplementary is available online free of charge and include the structural characterization, nuclear magnetic resonance data (^{1}H, ^{19}F and 2D NMR), details about electrochemical, calculation settings, transient absorption spectroscopy and spectroelectrochemistry measurements are provided as well as additional references.

8 References

[1] D. Gust, T.A. Moore, A.L. Moore, Molecular Mimicry of Photosynthetic Energy and Electron Transfer, Acc. Chem. Res. 26 (1993) 198–205, https://doi.org/10.1021/ar00028a010.
[2] M.R. Wasielewski, Photoinduced Electron Transfer in Supramolecular Systems for Artificial Photosynthesis, Chem. Rev. 92 (1992) 435–461, https://doi.org/10.1021/cr00011a005.
[3] D. Gust, T.A. Moore, A.L. Moore, Mimicking Photosynthetic Solar Energy Transduction, Acc. Chem. Res. 34 (2001) 40–48, https://doi.org/10.1021/ar9801301.
[4] S.-.C. Hung, A.N. Macpherson, S. Lin, P.A. Liddell, G.R. Seely, A.L. Moore, T. A. Moore, D. Gust, Coordinated Photoinduced Electron and Proton Transfer in a Molecular Triad, J. Am. Chem. Soc. 117 (1995) 1657–1658, https://doi.org/10.1021/ja00110a030.
[5] F. Lachaud, A. Quaranta, Y. Pellegrin, P. Dorlet, M.-.F. Charlot, S. Un, W. Leibl, A. Aukauloo, A Biomimetic Model of the Electron Transfer between P680 and the TyrZ–His190 Pair of PSII, Angew. Chemie Int. Ed. 44 (2005) 1536–1540, https://doi.org/10.1002/anie.200461948.
[6] J.D. Megiatto, A. Antoniuk-Pablant, B.D. Sherman, G. Kodis, M. Gervaldo, T. A. Moore, A.L. Moore, D. Gust, Mimicking the Electron Transfer Chain in Photosystem II with a Molecular Triad Thermodynamically Capable of Water Oxidation, Proc. Natl. Acad. Sci. 109 (2012) 15578–15583, https://doi.org/10.1073/pnas.1118348109.
[7] J.D. Megiatto Jr, D.D. Méndez-Hernández, M.E. Tejeda-Ferrari, A.-.L. Teillout, M. J. Llansola-Portolés, G. Kodis, O.G. Poluektov, T. Rajh, V. Mujica, T.L. Groy, D. Gust, T.A. Moore, A.L. Moore, A Bioinspired Redox Relay that Mimics Radical Interactions of the Tyr–His Pairs of Photosystem II, Nat. Chem. 6 (2014) 423–428, https://doi.org/10.1038/nchem.1862.
[8] C.J. Gagliardi, A.K. Vannucci, J.J. Concepcion, Z. Chen, T.J. Meyer, The Role of Proton Coupled Electron Transfer in Water Oxidation, Energy Environ. Sci. 5 (2012) 7704–7717, https://doi.org/10.1039/C2EE03311A.
[9] A.L. Balch, Y.S. Sohn, Oxidative-addition of *o*-Quinones to Ruthenium Complexes, J. Organomet. Chem. 30 (1971) C31–C32, https://doi.org/10.1016/S0022-328X(00)82584-X.
[10] L.R. Smith, D.M. Blake, D. Jackson, Coordinatively Unsaturated *o*-Quinone Complexes of Iridum(III) and their Role in the Isomerization of Octahedral Complexes, J. Organomet. Chem. 159 (1978) 409–415, https://doi.org/10.1016/S0022-328X(00)92226-5.
[11] S.R. Boone, C.G. Pierpont, Electron Distribution within Bis(quinone)ruthenium Complexes. Structural Characterization on Delocalized (Bipyridine)bis(quinone) ruthenium and on the Localized *trans*-Bis(3-chloropyridine)bis(3,5-*di*-tert-butyl-1,2-semiquinone)ruthenium(III) Cation, Polyhedron 9 (1990) 2267–2272, https://doi.org/10.1016/S0277-5387(00)86953-3.
[12] S. Bhattacharya, C.G. Pierpont, Structure and Bonding in Bis(quinone) Complexes of Ruthenium. Synthesis and Characterization of the $Ru(PPh_3)_2(SQ)_2$ (SQ = 3,5-tert-butylsemiquinone, tetrachloro-1,2-semiquinone) Series, Inorg. Chem. 30 (1991) 1511–1516, https://doi.org/10.1021/ic00007a017.
[13] N. Bag, A. Pramanik, G.K. Lahiri, A. Chakravorty, Chemistry of the Ruthenium [Ru(RQ)(tap)$_2$]z Family: Authentic Catecholates, Reduction Potentials, and Spectra (RQ = quinone/semiquinone/catecholate; tap = 2-(*m*-tolylazo)pyridine; z = 0, .+-., .+-.2), Inorg. Chem. 31 (1992) 40–45, https://doi.org/10.1021/ic00027a009.
[14] S. Bhattacharya, Synthesis, Characterization and Reactivity of a Ruthenium-Quinone Complex, Polyhedron 13 (1994) 451–456, https://doi.org/10.1016/S0277-5387(00)81659-9.
[15] M. Ebadi, A.B.P. Lever, Ruthenium Complexes of Quinone Related Ligands: A Study of the Electrochemical Properties of 2-Aminothiophenolatobis(2,2'-Bipyridine)Ruthenium(II), Inorg. Chem. 38 (1999) 467–474, https://doi.org/10.1021/ic980838b.
[16] C.G. Pierpont, Unique Properties of Transition Metal Quinone Complexes of the MQ3 Series, Coord. Chem. Rev. 219–221 (2001) 415–433, https://doi.org/10.1016/S0010-8545(01)00342-3.
[17] J. Yuasa, T. Suenobu, S. Fukuzumi, Binding Modes in Metal Ion Complexes of Quinones and Semiquinone Radical Anions: Electron-Transfer Reactivity, ChemPhysChem 7 (2006) 942–954, https://doi.org/10.1002/cphc.200500640.
[18] P.A. Abramov, N.P. Gritsan, E.A. Suturina, A.S. Bogomyakov, M.N. Sokolov, Rhenium Complex with Noninnocent Dioxolene Ligand: combined Experimental and ab Initio Study of [(3,5-di-tert-Bu2C6H2O2)ReCl3(OPPh3)], Inorg. Chem. 54 (2015) 6727–6735, https://doi.org/10.1021/acs.inorgchem.5b00407.
[19] R.B. Salmonsen, A. Abelleira, M.J. Clarke, S.D. Pell, Induced Electron Transfer in Ammineruthenium Catechol and Quinone Complexes, Inorg. Chem. 23 (1984) 385–387, https://doi.org/10.1021/ic00172a001.
[20] N.G. Connelly, I. Manners, J.R.C. Protheroe, M.W. Whiteley, Reduction–Oxidation Properties of Organotransition-Metal Complexes, Part 19. Carbonylruthenium catecholate and semiquinone complexes, J. Chem. Soc., Dalt. Trans. (1984) 2713–2717, https://doi.org/10.1039/DT9840002713.
[21] M. Haga, E.S. Dodsworth, A.B.P. Lever, S.R. Boone, C.G. Pierpont, Synthesis, Characterization, and Charge Distribution of bis(4-tert-butylpyridine)bis(3,5-di-tert-butylquinone)Ruthenium, J. Am. Chem. Soc. 108 (1986) 7413–7414, https://doi.org/10.1021/ja00283a049.
[22] W.P. Griffith, C.A. Pumphrey, T.-.A. Rainey, Catecholato Complexes of Ruthenium, Iridium, Rhenium, Molybdenum, and Tungsten, J. Chem. Soc., Dalt. Trans. (1986) 1125–1128, https://doi.org/10.1039/DT9860001125.
[23] M. Haga, E.S. Dodsworth, A.B.P. Lever, Catechol-Quinone Redox Series Involving bis(bipyridine)Ruthenium(II) and tetrakis(pyridine)Ruthenium(II), Inorg. Chem. 25 (1986) 447–453, https://doi.org/10.1021/ic00224a013.

[24] S.R. Boone, C.G. Pierpont, Charge Delocalization in Ruthenium-Quinone Complexes. Structural Characterization of Bis(bipyridine)(3,5-di-tert-butylsemiquinonato)ruthenium(II) Perchlorate and trans-Bis(4-tert-butylpyridine) bis(3,5-di-tert-butylquinone)ruthenium, Inorg. Chem. 26 (1987) 1769–1773, https://doi.org/10.1021/ic00258a027.
[25] A.B.P. Lever, P.R. Auburn, E.S. Dodsworth, M.A. Haga, W. Liu, M. Melnik, W. A. Nevin, Bis(dioxolene)(bipyridine)Ruthenium Redox Series, J. Am. Chem. Soc. 110 (1988) 8076–8084, https://doi.org/10.1021/ja00232a020.
[26] B.K. Ghosh, A. Chakravorty, Electrochemical Studies of Ruthenium Compounds Part I. Ligand Oxidation Levels, Coord. Chem. Rev. 95 (1989) 239–294, https://doi.org/10.1016/0010-8545(89)80027-X.
[27] M. Borgström, O. Johansson, R. Lomoth, H.B. Baudin, S. Wallin, L. Sun, B. Åkermark, L. Hammarström, Electron Donor−Acceptor Dyads and Triads Based on Tris(bipyridine)ruthenium(II) and Benzoquinone: Synthesis, Characterization, and Photoinduced Electron Transfer Reactions, Inorg. Chem. 42 (2003) 5173–5184, https://doi.org/10.1021/ic020606j.
[28] J. Hankache, D. Hanss, O.S. Wenger, Hydrogen-Bond Strengthening upon Photoinduced Electron Transfer in Ruthenium–Anthraquinone Dyads Interacting with Hexafluoroisopropanol or Water, J. Phys. Chem. A. 116 (2012) 3347–3358, https://doi.org/10.1021/jp300090n.
[29] K.A. Opperman, S.L. Mecklenburg, T.J. Meyer, Intramolecular, Photoinduced Electron Transfer in Ruthenium(II) Bipyridine-Quinone Complexes, Inorg. Chem. 33 (1994) 5295–5301, https://doi.org/10.1021/ic00101a022.
[30] J. Hankache, O.S. Wenger, Photoinduced Electron Transfer in Covalent Ruthenium–Anthraquinone Dyads: Relative Importance of Driving-force, Solvent Polarity, and Donor–bridge Energy Gap, Phys. Chem. Chem. Phys. 14 (2012) 2685–2692, https://doi.org/10.1039/C2CP23240E.
[31] J. Hankache, M. Niemi, H. Lemmetyinen, O.S. Wenger, Photoinduced Electron Transfer in Linear Triarylamine–Photosensitizer–Anthraquinone Triads with Ruthenium(II), Osmium(II), and Iridium(III), Inorg. Chem. 51 (2012) 6333–6344, https://doi.org/10.1021/ic300558s.
[32] M. Kuss-Petermann, O.S. Wenger, Electron Transfer Rate Maxima at Large Donor–Acceptor Distances, J. Am. Chem. Soc. 138 (2016) 1349–1358, https://doi.org/10.1021/jacs.5b11953.
[33] A. Dey, J. Dana, S. Aute, A. Das, H.N. Ghosh, Hydrogen Bond Assisted Photoinduced Intramolecular Electron Transfer and Proton Coupled Electron Transfer in an Ultrafast Time Domain Using a Ruthenium-Anthraquinone Dyad, Photochem. Photobiol. Sci. 18 (2019) 2430–2441, https://doi.org/10.1039/C9PP00135B.
[34] R. Díaz, A. Francois, M. Barrera, B. Loeb, Synthesis, Characterization and Theoretical Studies of Ruthenium(II) Complexes with the Quinone Functionalized Polypyridine Ligand, Nqphen, Polyhedron. 39 (2012) 59–65, https://doi.org/10.1016/j.poly.2012.03.020.
[35] J.C. Deaton, F.N. Castellano, Archetypal Iridium(III) Compounds for Optoelectronic and Photonic Applications, Iridium(III) Optoelectron. Photonics Appl. (2017) 1–69, https://doi.org/10.1002/9781119007166.ch1.
[36] J.M. Younker, K.D. Dobbs, Correlating Experimental Photophysical Properties of Iridium(III) Complexes to Spin–Orbit Coupled TDDFT Predictions, J. Phys. Chem. C. 117 (2013) 25714–25723, https://doi.org/10.1021/jp410576a.
[37] E. Pomarico, M. Silatani, F. Messina, O. Braem, A. Cannizzo, E. Barranoff, J. H. Klein, C. Lambert, M. Chergui, Dual Luminescence, Interligand Decay, and Nonradiative Electronic Relaxation of Cyclometalated Iridium Complexes in Solution, J. Phys. Chem. C. 120 (2016) 16459–16469, https://doi.org/10.1021/acs.jpcc.6b04896.
[38] J.-.H. Kim, S.-.Y. Kim, Y.-.J. Cho, H.-.J. Son, D.W. Cho, S.O. Kang, A Detailed Evaluation for the Nonradiative Processes in Highly Phosphorescent Iridium(III) Complexes, J. Phys. Chem. C. 122 (2018) 4029–4036, https://doi.org/10.1021/acs.jpcc.7b12449.
[39] J.-.H. Kim, S.-.Y. Kim, S. Jang, S. Yi, D.W. Cho, H.-.J. Son, S.O. Kang, Blue Phosphorescence with High Quantum Efficiency Engaging the Trifluoromethylsulfonyl Group to Iridium Phenylpyridine Complexes, Inorg. Chem. 58 (2019) 16112–16125, https://doi.org/10.1021/acs.inorgchem.9b02672.
[40] L. Wang, S. Monro, P. Cui, H. Yin, B. Liu, C.G. Cameron, W. Xu, M. Hetu, A. Fuller, S. Kilina, S.A. McFarland, W. Sun, Heteroleptic Ir(III)N6 Complexes with Long-Lived Triplet Excited States and *in Vitro* Photobiological Activities, ACS Appl. Mater. Interfaces. 11 (2019) 3629–3644, https://doi.org/10.1021/acsami.8b14744.
[41] S. DiLuzio, V. Mdluli, T.U. Connell, J. Lewis, V. VanBenschoten, S. Bernhard, High-Throughput Screening and Automated Data-Driven Analysis of the Triplet Photophysical Properties of Structurally Diverse, Heteroleptic Iridium(III) Complexes, J. Am. Chem. Soc. 143 (2021) 1179–1194, https://doi.org/10.1021/jacs.0c12290.
[42] S. Neumann, C. Kerzig, O.S. Wenger, Quantitative Insights into Charge-Separated States from One- and Two-Pulse Laser Experiments Relevant for Artificial Photosynthesis, Chem. Sci. 10 (2019) 5624–5633, https://doi.org/10.1039/C9SC01381D.
[43] L. Sun, Y. Chen, S. Kuang, G. Li, R. Guan, J. Liu, L. Ji, H. Chao, Iridium(III) Anthraquinone Complexes as Two-Photon Phosphorescence Probes for Mitochondria Imaging and Tracking under Hypoxia, Chem. – A Eur. J. 22 (2016) 8955–8965, https://doi.org/10.1002/chem.201600310.
[44] T. Maehara, R. Kanno, S. Yokoshima, T. Fukuyama, A Practical Preparation of Highly Versatile *N*-Acylpyrroles from 2,4,4-Trimethoxybutan-1-amine, Org. Lett. 14 (2012) 1946–1948, https://doi.org/10.1021/ol3005613.
[45] A. Singh, K. Teegardin, M. Kelly, K.S. Prasad, S. Krishnan, J.D. Weaver, Facile Synthesis and Complete Characterization of Homoleptic and Heteroleptic Cyclometalated Iridium(III) Complexes for Photocatalysis, J. Organomet. Chem. 776 (2015) 51–59, https://doi.org/10.1016/j.jorganchem.2014.10.037.
[46] J. Ma, X. Zhang, X. Huang, S. Luo, E. Meggers, Preparation of Chiral-at-Metal Catalysts and their use in Asymmetric Photoredox Chemistry, Nat. Protoc. 13 (2018) 605–632, https://doi.org/10.1038/nprot.2017.138.
[47] D. Gust, T.A. Moore, A.L. Moore, G. Seely, P. Liddell, D. Barrett, L.O. Harding, X. C. Ma, S.-.J. Lee, F. Gao, A Carotenoid-Porphyrin-*di*Quinone Tetrad: Synthesis, Electrochemistry and Photoinitiated Electron Transfer, Tetrahedron 45 (1989) 4867–4891, https://doi.org/10.1016/S0040-4020(01)85157-7.
[48] H. Sayre, H.H. Ripberger, E. Odella, A. Zieleniewska, D.A. Heredia, G. Rumbles, G. D. Scholes, T.A. Moore, A.L. Moore, R.R... Knowles, PCET-Based Ligand Limits Charge Recombination with an Ir(III) Photoredox Catalyst, J. Am. Chem. Soc. 143 (2021) 13034–13043, https://doi.org/10.1021/jacs.1c01701.
[49] M.S. Lowry, J.I. Goldsmith, J.D. Slinker, R. Rohl, R.A. Pascal, G.G. Malliaras, S. Bernhard, Single-Layer Electroluminescent Devices and Photoinduced Hydrogen Production from an Ionic Iridium(III) Complex, Chem. Mater. 17 (2005) 5712–5719, https://doi.org/10.1021/cm051312+.
[50] L.F. Fieser, M. Fieser, The Reduction Potentials of Various Naphthoquinones, J. Am. Chem. Soc. 57 (1935) 491–494, https://doi.org/10.1021/ja01306a031.
[51] Y. Tawada, T. Tsuneda, S. Yanagisawa, T. Yanai, K. Hirao, A Long-Range-Corrected Time-Dependent Density Functional Theory, J. Chem. Phys. 120 (2004) 8425–8433, https://doi.org/10.1063/1.1688752.
[52] J.-.D. Chai, M. Head-Gordon, Systematic Optimization of Long-Range Corrected Hybrid Density Functionals, J. Chem. Phys. 128 (2008) 84106, https://doi.org/10.1063/1.2834918.
[53] F. Strieth-Kalthoff, C. Henkel, M. Teders, A. Kahnt, W. Knolle, A. Gómez-Suárez, K. Dirian, W. Alex, K. Bergander, C.G. Daniliuc, B. Abel, D.M. Guldi, F. Glorius, Discovery of Unforeseen Energy-Transfer-Based Transformations Using a Combined Screening Approach, Chem. 5 (2019) 2183–2194, https://doi.org/10.1016/j.chempr.2019.06.004.
[54] R. Sun, Y. Qin, S. Ruccolo, C. Schnedermann, C. Costentin, D.G. Nocera, Elucidation of a Redox-Mediated Reaction Cycle for Nickel-Catalyzed Cross Coupling, J. Am. Chem. Soc. 141 (2019) 89–93, https://doi.org/10.1021/jacs.8b11262.
[55] S.-.H. Lee, C.T.-L. Chan, K.M.-C. Wong, W.H. Lam, W.-.M. Kwok, V.W.-W. Yam, Synthesis and Photoinduced Electron Transfer in Platinum(II) bis(*N*-(4-ethynylphenyl)carbazole)Bipyridine Fullerene Complexes, Dalt. Trans. 43 (2014) 17624–17634, https://doi.org/10.1039/C4DT01397B.
[56] G. Angulo, A. Rosspeintner, B. Lang, E. Vauthey, Optical Transient Absorption Experiments Reveal the Failure of Formal Kinetics in Diffusion Assisted Electron Transfer Reactions, Phys. Chem. Chem. Phys. 20 (2018) 25531–25546, https://doi.org/10.1039/C8CP05153D.
[57] G. Angulo, A. Rosspeintner, Bimolecular Photo-Induced Electron Transfer Enlightened by Diffusion, J. Chem. Phys. 153 (2020) 40902, https://doi.org/10.1063/5.0014384.
[58] A.J. Musacchio, L.Q. Nguyen, G.H. Beard, R.R. Knowles, Catalytic Olefin Hydroamination with Aminium Radical Cations: a Photoredox Method for Direct C–N Bond Formation, J. Am. Chem. Soc. 136 (2014) 12217–12220, https://doi.org/10.1021/ja5056774.
[59] G.J. Choi, R.R. Knowles, Catalytic Alkene Carboaminations Enabled by Oxidative Proton-Coupled Electron Transfer, J. Am. Chem. Soc. 137 (2015) 9226–9229, https://doi.org/10.1021/jacs.5b05377.
[60] K.T. Tarantino, P. Liu, R.R. Knowles, Catalytic Ketyl-Olefin Cyclizations Enabled by Proton-Coupled Electron Transfer, J. Am. Chem. Soc. 135 (2013) 10022–10025, https://doi.org/10.1021/ja404342j.
[61] E.C. Gentry, R.R. Knowles, Synthetic Applications of Proton-Coupled Electron Transfer, Acc. Chem. Res. 49 (2016) 1546–1556, https://doi.org/10.1021/acs.accounts.6b00272.